Intravenous Injection of Clinical Grade Human MSCs After Experimental Stroke: Functional Benefit and Microvascular Effect

Anaïck Moisan,*†‡ Isabelle Favre,*†§ Claire Rome,*† Florence De Fraipont,¶# Emmanuelle Grillon,*†
Nicolas Coquery,*† Hervé Mathieu,*† Virginie Mayan,*† Bernadette Naegele,*†§ Marc Hommel,**
Marie-Jeanne Richard,‡¶# Emmanuel Luc Barbier,*† Chantal Remy,*† and Olivier Detante*†§

*The French National Institute of Health and Medical Research (Inserm), Grenoble, France
†Université Grenoble Alpes, Grenoble, France
‡French Blood Company/CHU de Grenoble, Hôpital Michallon, Unité de Thérapie et d'Ingénierie Cellulaire, Saint Ismier, France
§Unité Neurovasculaire, Département de Neurologie, Hôpital Michallon, CHU Grenoble Alpes, Grenoble, France
¶UM Biochimie des Cancers et Biothérapies, Hôpital Michallon, CHU Grenoble Alpes, Grenoble, France
#Institut Albert Bonniot, Inserm, Université Grenoble Alpes, Grenoble, France
**Département de Recherche Clinique, Hôpital Michallon, CHU de Grenoble, Grenoble, France

Stroke is the leading cause of disability in adults. Many current clinical trials use intravenous (IV) administration of human bone marrow-derived mesenchymal stem cells (BM-MSCs). This autologous graft requires a delay for ex vivo expansion of cells. We followed microvascular effects and mechanisms of action involved after an IV injection of human BM-MSCs (hBM-MSCs) at a subacute phase of stroke. Rats underwent a transient middle cerebral artery occlusion (MCAo) or a surgery without occlusion (sham) at day 0 (D0). At D8, rats received an IV injection of 3 million hBM-MSCs or PBS-glutamine. In a longitudinal behavioral follow-up, we showed delayed somatosensory and cognitive benefits 4 to 7 weeks after hBM-MSC injection. In a separate longitudinal in vivo magnetic resonance imaging (MRI) study, we observed an enhanced vascular density in the ischemic area 2 and 3 weeks after hBM-MSC injection. Histology and quantitative polymerase chain reaction (qPCR) revealed an overexpression of angiogenic factors such as Ang1 and transforming growth factor-β1 (TGF-β1) at D16 in hBM-MSC-treated MCAo rats compared to PBS-treated MCAo rats. Altogether, delayed IV injection of hBM-MSCs provides functional benefits and increases cerebral angiogenesis in the stroke lesion via a release of endogenous angiogenic factors enhancing the stabilization of newborn vessels. Enhanced angiogenesis could therefore be a means of improving functional recovery after stroke.

Key words: Mesenchymal stem cells (MSCs); Cell therapy; Cerebral ischemia; Stroke; Microvasculature; Angiogenesis

INTRODUCTION

Stroke is the leading cause of acquired adult disability. There are currently no effective treatments for ischemic stroke beyond the first 4.5 h (the therapeutic window for thrombolysis) except rehabilitation. To enhance tissue repair and thereby reduce disability, cell therapies are currently being developed[1]. In this field, bone marrow-derived mesenchymal stem cells (BM-MSCs) are attractive as they are not derived from a tumoral or modified source. Moreover, they are weakly immunogenic[2], they can be expanded in culture, and they can be administered under autologous conditions.

In stroke models, the benefits of human MSC (hMSC) administration for functional recovery are well established at the acute phase of stroke (between 3 h and 3 days)[1]. Neuroprotective and immunomodulatory effects have been shown after early intravenous (IV)[3–7] and intracerebral (IC)[8] injection of hMSCs. A proangiogenic effect has been demonstrated after IV injections of BM-MSCs[5,9–13], human umbilical cord blood-derived MSCs (hUCB-MSCs)[14–16], or adipose tissue-derived MSCs (ADSCs)[17].

The results of four pilot clinical trials suggested a good tolerance of IV-injected autologous hMSCs in patients[18–20]. An autologous injection of cells requires a

delay (several days) to isolate, expand, and control cells. Therefore, therapeutic injection of autologous cells is necessarily performed at the subacute phase of stroke. However, limited data are available about the impact of hMSCs injected at this subacute stage. In animal models, two studies showed a functional benefit of IC and IV injection of hUCB-MSCs at 7 days[14,21] and IV infusion 30 days following injury[21]. The use of rat-derived MSCs was also investigated at the subacute stage of stroke but yielded controversial results[22–29]. Five studies investigated the mechanisms of action of hUCB-MSCs, cryopreserved BM-MSCs, and rat MSCs. Three studies revealed a proangiogenic effect[25,29,30], and two other studies showed an improvement in neurogenesis[22,26].

To date, the effects of a delayed (beyond 3 days) IV injection of freshly isolated BM-MSCs for stroke remain unknown. The subacute stage is, however, an active phase during which microvascular remodeling and neurogenesis occur[31]. Thus, the purpose of this study was to assess functional benefits and microvascular effects of IV-injected human BM-MSCs (hBM-MSCs) at the subacute phase in a rat model of ischemic stroke.

MATERIALS AND METHODS

All procedures were conducted according to French guidelines on the use of animals for scientific investigations (permits 380820 for CR, 381106 for AM, and A3851610008 for the facilities) with ethical committee approval (Grenoble Institute of Neurosciences agreement 004). A total of 78 male Sprague–Dawley (SD) rats weighing 280–330 g (7–8 weeks old) (Janvier Labs, Le Genest Saint Isle, France) were used for this study [25 rats for behavioral study, 26 rats for magnetic resonance imaging (MRI) microvascular follow-up, and 27 rats for biological ex vivo study]. For surgery and MRI, anesthesia was induced by inhalation of 5% isoflurane (Abbott Scandinavia AB, Solna, Sweden) in 30% O_2 and maintained throughout all surgical and imaging procedures with 2–2.5% isoflurane through a facial mask. Rectal temperature was monitored and maintained at 37.0±0.5°C.

Transient Middle Cerebral Artery Occlusion (MCAo) Model

Male SD rats weighing 280–330 g underwent surgery at day 0 (D0). Transient focal brain ischemia was induced by intraluminal MCAo according to our previously described method using commercially made silicon rubber-coated monofilaments (0.37-mm diameter; Doccol Corporation, Redlands, CA, USA)[32]. After 90 min of occlusion, rats were functionally assessed then reanesthetized to remove the thread. The sham-operated rats underwent the same procedure without MCAo. Hemorrhagic (visualized by MRI) and partial lesions (only striatal or cortical) were excluded from our study.

Experimental Groups and IV Administration of Human BM-MSCs (hBM-MSCs)

IV administration was performed via the tail vein by a blinded operator. No immunosuppressive drugs were used.

Behavioral Study. Twenty-five rats underwent MCAo at D0 and were randomly allocated into two groups, with a stratification based on initial MRI lesion volume. At D8, rats received an IV injection of either 1 ml phosphate-buffered saline (PBS)-glutamine (Thermo Fisher Scientific, Waltham, MA, USA) (group MCAo-PBS, $n=12$) or 3 million iron-labeled hBM-MSCs (group MCAo-hBM-MSCs, $n=13$). These rats underwent a 7-week MRI and behavioral follow-up (Fig. 1A), at the end of which they were sacrificed, and major organs (brain, liver, spleen, lungs, and muscle) were excised for immunohistochemistry (IHC). Animals were imaged with MRI at D2, D10, week 5 (W5), and W7.

Microvascular Study. For MRI follow-up (Fig. 1B), 26 rats were randomly allocated into three groups. Rats underwent MCAo at D0 and at D8 received an IV injection of 1 ml of PBS-glutamine (group MCAo-PBS MRI, $n=8$) or 3 million hBM-MSCs (group MCAo-hBM-MSC MRI, $n=9$). Sham-operated rats received, at D8, 1 ml of PBS-glutamine via IV injection (group sham MRI, $n=9$). All animals were imaged by MRI at D3, D7, D9, and D16 and, due to technical limitations, only five rats per group at D25. For biological follow-up, 24 additional MCAo rats were deeply anesthetized with isoflurane and decapitated for ex vivo experiments. Before hBM-MSC injection, three MCAo rats were analyzed at each time point, and after hBM-MSC injection, three were obtained for the MCAo-PBS group and three for the MCAo-hBM-MSC group at each time point. In addition, three sham rats were euthanized at D25 and used as a reference for reverse transcription quantitative polymerase chain reaction (qPCR) experiments.

hBM-MSC Culture and Labeling

Clinical-grade hBM-MSCs were used to be consistent with the ongoing clinical trial in our center [Intravenous Stem Cells After Ischemic Stroke (ISIS), NCT00875654]. hMSCs were isolated from BM aspirate from four healthy donors who gave their written informed consent, and all procedures were in compliance with the French public health code (Article L1241-1) (Table 1). Culture procedures were conducted according to previously described methods[32,33].

To evaluate the presence of hBM-MSCs in the tissue, cells were labeled with micrometer-sized fluorescent and superparamagnetic iron oxide (SPIO) particles[34]. Particles [iron fluorescent particles (IFPs); Bangs Laboratory, Fishers, IN, USA] had a carboxylated iron oxide core
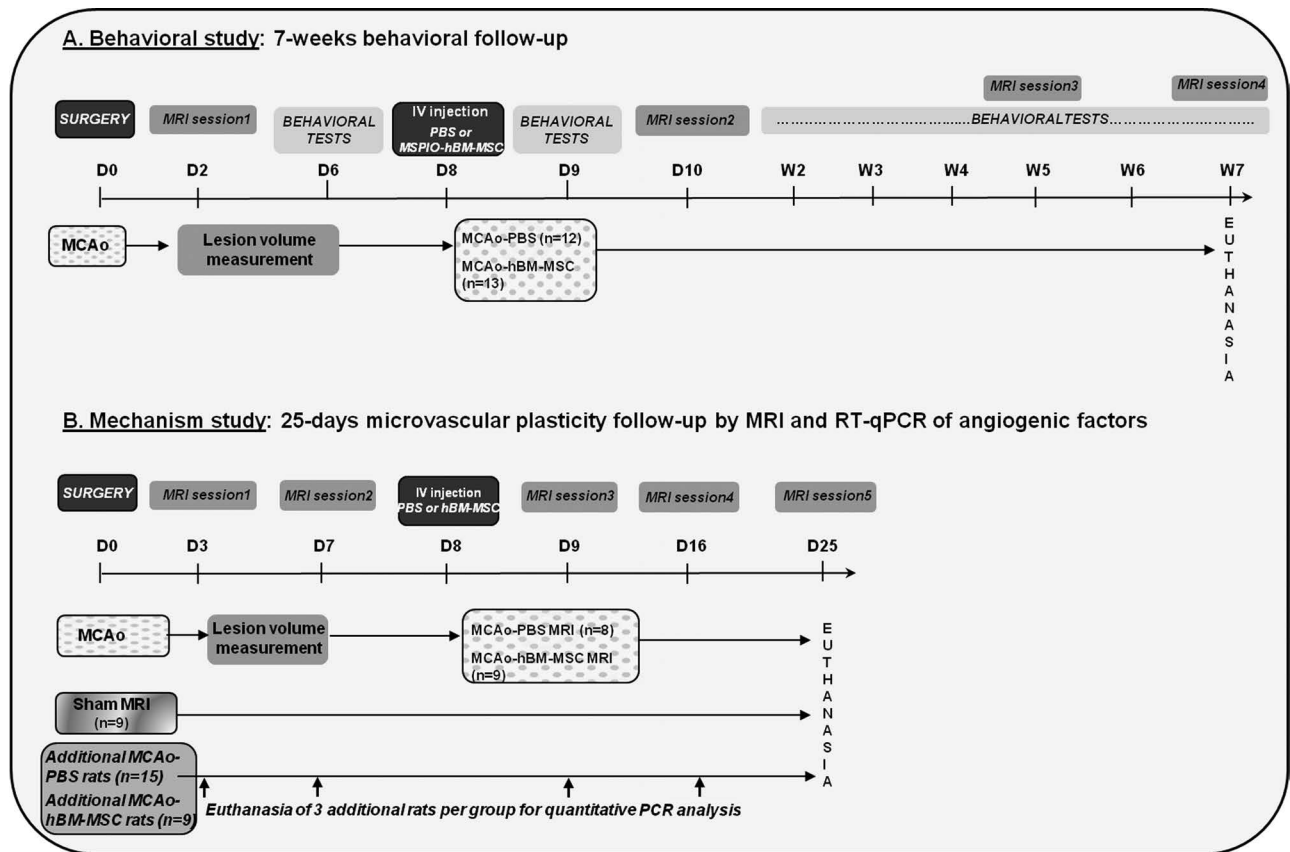
Figure 1. Study design. (A) Behavioral study. Rats underwent a behavioral follow-up for 7 weeks after middle cerebral artery occlusion (MCAo). (B) Mechanism study. Rats were imaged by magnetic resonance imaging (MRI) for 25 days following MCAo. Additional rats were euthanized at each time point to perform analysis of angiogenic factors.

(diameter = 0.9 μm; 63.4% magnetite w/w) and carried "dragon green" fluorophores (excitation wavelength = 480 nm; emission = 520 nm), enabling in vivo MRI and ex vivo optical detection. Briefly, hBM-MSCs from a second passage were incubated for 20 h at 37°C in 5% CO_2 with SPIO (final concentration in culture medium: 12.7 μg Fe/ml). After incubation, hBM-MSCs were washed twice with PBS to remove particles that had not been taken up, and were then cultured or trypsinized (trypsin; Thermo Fisher Scientific). This SPIO labeling is known to preserve

viability, phenotype, and ability of BM-MSCs to differentiate into mesodermal lineage tissues[34].

For the microvascular study, native hBM-MSCs were harvested after two passages for IV injection.

Behavioral Tests

Behavioral tests were carried out by a blinded operator at D6, D9, W2, W3, W4, W5, W6, and W7 after surgery. Rats were subjected to somatosensory tests widely used in stroke models: modified neurological severity score (mNSS) and adhesive removal test (ART). Rats were familiarized with the testing environment and trained for 3 days (three trials a day for each test) before MCAo. The mNSS scores include a combination of motor, sensory, balance, and reflex tests [between 0 (normal) and 18 (maximal deficit]. The ART score was used to assess the asymmetry in dexterity and sensitivity; an adhesive-backed paper dot (1 cm^2) was applied on each front paw. Three trials per rat were performed, and the mean time to remove each adhesive was measured with a maximum delay of 120 s.

As cognitive functions, such as spatial memory, remain impaired for at least 2 months after experimental

Table 1. Characteristics of the Bone Marrow Donors

Study	Age of Donors	Gender of Donors
Behavioral study		
Donor 1	15 years old	Male
Donor 2	58 years old	Male
Microvascular and biological study		
Donor 1	13 years old	Male
Donor 2	48 years old	Female

stroke[35,36], spatial memory was assessed using an eight-arm radial maze (RAM; Bioseb, Vitrolles, France) with a delayed match to sample task (win–stay strategy). Rats were trained for RAM for 3 weeks (5 days per week) before the experiment. Animals underwent a 12-h food restriction before each trial. Small pellets (Smacks; Kellogs SA, Bobigny, France) were located in cups at the ends of three nonadjacent arms. The five empty arms were blocked off to force the rats to explore the three accessible, baited arms. Rats had to find the three pellets, and the time to complete this session, so-called "predelay session," was noted (maximum allowed time for this session: 5 min). Rats were then placed on the central ring under a black box for a delay of 30 s. The same three baited arms were rebaited, and all eight arms were opened. During this session, so-called "postdelay session," rats were then allowed to freely select arms until they found the three pellets. Time to complete this session (maximum allowed time: 5 min), number of errors including entries into a nonbaited arm, and reentries into an already explored arm (perseverations) were noted.

*In Vivo Multiparametric MRI
Experiments and Analysis*

MRI was performed on a 7T spectrometer (Advance III; Bruker, Billerica, MA, USA) at the MRI facility of Grenoble, France (IRMaGe).

Behavioral Study. The 25 rats, MCAo-PBS ($n=12$) and MCAo-hBM-MSC ($n=13$) groups, were examined by MRI over a period of 7 weeks (D2, D10, W5, and W7). T_2-weighted (T_2W) images [spin echo, repetition time/echo time (TR/TE) $=2,500/60$ ms, voxel size $=234 \times 234 \times 1,000$ μm^3] were used to measure the lesion volume. T_2*-weighted (T_2*W) images (gradient echo, TR $=5,000$ ms, six echoes from 6 to 38 ms, voxel size $=234 \times 234 \times 1,000$ μm^3) were used to detect the SPIO-labeled hBM-MSCs.

Microvascular Study. MCAo-PBS ($n=8$), MCAo-hBM-MSC ($n=9$), and sham ($n=9$) groups were examined by MRI at D3, D7, D9, D16, and D25. Breathing rates were maintained at 45–50 breaths per minute during each MRI session by regulation of the anesthesia level. T_2W images (TR/TE $=2,500/60$ ms, voxel size $=234 \times 234 \times 1,000$ μm) were acquired to measure lesion volume. Cerebral blood volume (CBV), vessel size index (VSI; mean perfused vessel caliber), and vascular density imaging were analyzed using a steady-state approach[32,37,38]. This technique relies on the change in transverse relaxation rates (T_2 for spin echo and T_2* for gradient echo) induced by an intravascular contrast agent and produces robust quantitative maps of the microvascular characteristics mentioned above. Several comparisons between microvascular estimates obtained by MRI and by a reference technique

were performed by several groups worldwide, as recently reviewed by Tropres et al.[39]. Briefly, a multi gradient echo-spin echo sequence (TR $=4,000$ ms; spin echo $=40$ ms, seven gradient echoes from 2.3 to 15.6 ms; voxel size, $234 \times 234 \times 1,000$ μm^3; seven slices) was performed, before and 2 min after IV injection (tail vein) of an intravascular iron-based contrast agent (200 μmol iron/kg body weight, 389.8 μl/kg body weight; P904; Guerbet, Roissy, France). Blood–brain barrier (BBB) leakage was assessed using T_1W images (TR/TE $=300/4.8$ ms) acquired before and 3 min after IV injection of 0.2 mmol/kg Gd-1,4,7,10-tetraazacyclododecane-1,4,7,10-tetraacetic acid (400 μl/kg body weight; DOTA; Dotarem; Guerbet).

MRI Data Analysis. The region of interest (ROI) corresponding to the whole ischemic lesion was manually delineated by a blinded operator on T_2W images as previously described[32]. In sham rats, an ipsilateral ROI was drawn to obtain a volume equal to the mean lesion volume of the MCAo group for each MRI session.

CBV and VSI maps were computed using homemade software developed within Matlab (MathWorks, Natick, MA, USA), according to Tropres et al.[37]. Vascular density per mm^2 (N) was derived from the ratio ($[\Delta R_2/(\Delta R_2^*)^{2/3}]$) according to equation 7 of Wu et al.[40]. CBV, VSI, and vascular density were measured in the same ROI, from nonexcluded pixels [pixels were excluded in case of erroneous fitting (CBV $<0\%$) or when outside the validity range of the method, i.e., CBV $> 17\%$, VSI > 50 μm]. These parameters (CBV, VSI, and N) reflect only functional (i.e., circulating) vessels[41].

BBB permeability was calculated on the T_1W images as the signal enhancement (SE; %) induced by Gd-DOTA extravasation, according to the ratio: [SI$_{after Gd\_DOTA}$ − SI$_{before Gd\_DOTA}$]/SI$_{before Gd\_DOTA}$, where SI is the signal intensity.

SYBR Green Real-Time qPCR

Total RNA was extracted from frozen hemispheres with TRIzol reagent (Invitrogen, Life Technologies Ltd., Paisley, UK) using a MagNA Lyser (Roche, Indianapolis, IN, USA). Total RNA quantification was performed on a spectrophotometer (NanoDrop ND2000; Thermo Fisher Scientific). Reverse transcription was performed under conditions recommended by the manufacturers (GoScript; Promega, Madison, WI, USA). Thirteen primers were designed using the Primer3 program (Whitehead Institute for Biomedical Research, Cambridge, MA, USA) (Table 2), and qPCR was performed on a Stratagene Thermocycler (Agilent Technologies, Massy, France) using the SYBR Green (Thermo Fisher Scientific) method[42]. Specificity of each PCR product was assessed using the dissociation reaction plot. Relative gene expression was calculated with the $2^{-\Delta\Delta CT}$ method using the level of

Table 2. Oligonucleotides Used for Quantitative Reverse Transcription Polymerase Chain Reaction (RT-qPCR)

Role/cDNA	Primer Sequence (5′-3′)	Product (bp)
Proliferation		
FGF-2	TCTTCCTGCGCATCCATC GCTTGGAGCTGTAGTTTGACG	82
VEGF-A	GCTGTGTGTGTGAGTGGCTTA CCCATTGCTCTGTACCTTGG	61
VEGFR-1	CAGTTTCCAAGTGGCCAGAG AGGTCGCGATGAATGCAC	63
VEGFR-2	GGAGATTGAAAGAAGGAACGAG TGGTACATTTCTGGGGTGGT	61
Ang2	CAAGTGTTCCCAGATGCTCA AAGTTGGAAGGACCACATGC	60
eNOS	TGACCCTCACCGATACAACA CGGGTGTCTAGATCCATGC	60
Stabilization and maturation		
Ang1	ATGCGCCCTTATGCTAACAG TTTAGATTGGAAGGGCCACA	60
Tie1	CAGCGTCTACACTACCAAGAGTG CCTCCAAGGCTCACTATCTCC	72
Tie2	CATAGGAGGAAACCTGTTCACC CCCACTTCTGAGCTTCACATC	71
TGF-β1	GTCAACTGTGGAGCAACACG GACAGCCACTCAGGCGTATC	108
Chemoattraction		
SDF-1	GTGTTCCTACCCCCAAGGAT TGGTGGGATGAAGAGGAGAG	110
CXCR-4	GCATCATCATCTCCAAGCTG GAAGGAATCGATGCTGATCC	134
Housekeeping		
GAPDH	GGCTCTCTGCTCCTCCCTGTTCTA TACGGCCAAATCCGTTCACACCGA	107

Ang1, angiopoietin 1; Ang2, angiopoietin 2; CXCR-4, chemokine receptor type 4; eNOs, endothelial nitric oxide synthase; FGF-2, fibroblast growth factor 2; GAPDH, glyceraldehyde-3-phosphate dehydrogenase; SDF-1, stromal-derived factor-1; TGF-β1, transforming growth factor-β1; VEGF, vascular endothelial growth factor.
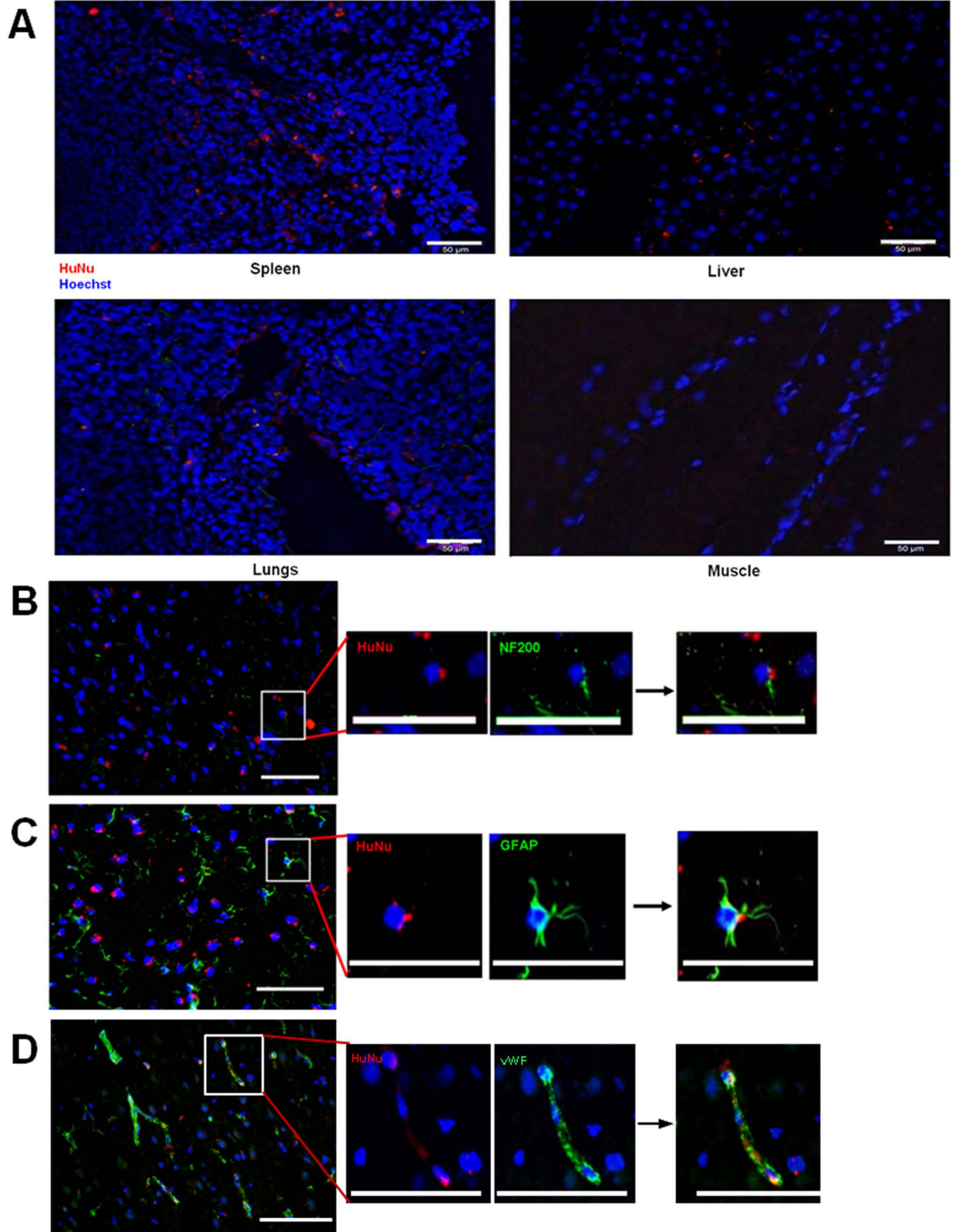
glyceraldehyde-3-phosphate dehydrogenase (GAPDH) expression and the expression levels of sham samples as normalization factors. Samples were duplicated for each gene analysis.

Immunohistochemistry

Brains were removed, frozen, and stored at −80°C. Frozen sections (12 μm thick) were incubated overnight at 4°C with primary antibodies, washed with PBS, and incubated (1 h) at room temperature with secondary antibodies. SPIO provided a direct fluorescent label for microscopy [fluorescein isothiocyanate (FITC) like]. Human BM-MSCs were identified by anti-human nuclei monoclonal antibody (HuNu; 1:2,000; MAB1281; Chemicon Int., Billerica, MA, USA). Cell differentiation into neurons was assessed with an anti-neurofilament antibody (rabbit anti-NF200, N4142; 1:500; Sigma-Aldrich, St. Louis, MO, USA), into astrocytes with anti-glial fibrillary acidic protein (rabbit anti-GFAP, 20334; 1:500; Dako, Les Ulis, France), and into endothelial cells with anti-von Willebrand factor (vWF; rabbit anti-factor VIII; 1:500; Dako). An FITC donkey anti-mouse immunoglobulin G (IgG; 1:500; Invitrogen) and a rhodamine-conjugated donkey anti-rabbit IgG (1:200; Jackson ImmunoResearch, West Grove, PA, USA) were used, respectively, for double-label immunoreactivity. Images were obtained using epifluorescence microscopy (Nikon Eclipse E600; Nikon, Tokyo, Japan) and a charge-coupled device (CCD) camera (Olympus, Rungis, France). Cell nuclei were visualized using blue fluorescent Hoechst 33342 counterstaining (Gelmount, Microm Microtech, Brignais, France) containing Hoechst 33342 trichlorohydride (1 μg/ml).

Four ROIs analyzed in each rat were (i) the striatum in the ipsilateral hemisphere, (ii) the subcortical area in

HuNu
Hoechst

Spleen   Liver

Lungs   Muscle

the ipsilateral hemisphere, (iii) the striatum in the contralateral hemisphere, and (iv) the subcortical area in the contralateral hemisphere. HuNu-positive cells were counted in each ROI using ImageJ software [Nucleus Counter Tool; ImageJ; National Institutes of Health (NIH), Bethesda, MD, USA]. Quantification is reported as the ratio of HuNu-positive cells over the total number of nuclei in the field of view.

Statistical Analysis

All analyses were blindly performed. Results are expressed as mean ± standard error of the mean (SEM) for behavioral and qPCR data, and as mean ± standard deviation (SD) for MRI data. Mean values were kept in the article to homogenize the data presentation for ease of interpretation. For analyzing repeated measures during behavioral follow-up, repeated-measures analysis of variance (ANOVA) was applied after testing variance homogeneity (Levene's test). Bonferroni post hoc tests were used for p value adjustment. Paired t-tests were used for within-group comparison at each time point. A Mann–Whitney U test was used for MRI between-group comparisons and qPCR analysis. A value of $p \leq 0.05$ was considered significant. Nonparametric tests were done on rank data. All data were analyzed using SPSS software (SPSS Statistics v20; IBM, Armonk, NY, USA).

RESULTS

Human BM-MSCs Were Well Tolerated After IV Injection With a Long-Term Cell Survival in Organs

No adverse effect was observed after IV injection of hBM-MSCs. No tumoral lesion was observed in the brain, liver, spleen, lungs, or muscle of hBM-MSC- or PBS-treated rats.

At the end of the follow-up, some HuNu-positive human cells were observed in the brain, liver, spleen, and lungs of all MCAo-hBM-MSC rats, but not in muscles (Fig. 2A). No HuNu-positive cells were observed in the brains or peripheral organs from the MCAo-PBS group (data not shown). We were not able to distinguish microbleeds (small foci of blood in tissue) by our T_2^* MRI technique from SPIO labeling (data not shown). SPIO fluorescence was detected in the brain of only 1 rat out of 13 from the MCAo-hBM-MSC group. This enabled us to perform double immunolabeling of HuNu-positive cells (human cells) with rhodamine and FITC on adjacent cells. We observed that human cells

rarely differentiated into astrocytes (HuNu/GFAP), neurons (HuNu/NF200), or endothelial cells (HuNu/vWF), notably around the cerebral infarction (Fig. 2B and C).

Human BM-MSC Therapy Improved Recovery

MCAo groups exhibited similar initial lesion volume and similar lesion evolution over 25 days for the MCAo MRI groups and over 7 weeks for the MCAo behavior group (data not shown). No significant effect of hBM-MSCs on lesion volume was observed. Cerebral injury was confirmed in all MCAo rats, which exhibited a high mNSS (Fig. 3A) and delay in removing adhesives on the left forelimb (Fig. 3B) over 7 weeks. We observed an increased sensorimotor recovery in the MCAo-hBM-MSC group compared to the MCAo-PBS group ($p = 0.007$). Sensorimotor recovery for ART was better after a longer delay following hBM-MSC injection (MCAo-hBM-MSC vs. MCAo-PBS at 5 weeks: 43.8 ± 27.4 s vs. 74.3 ± 34.2 s, $p = 0.031$).

Recovery of spatial memory was also improved in rats that received hBM-MSCs compared to PBS. A benefit was observed from 5 weeks after stroke (i.e., 4 weeks following hBM-MSC injection) with a sustained effect until 7 weeks (Fig. 4A–D). The predelay session (period where the rats learn the task at the beginning of the behavioral session) revealed that MCAo-hBM-MSC rats took less time to complete the "learning" task from 5 to 7 weeks (MCAo-hBM-MSC vs. MCAo-PBS at W5: 58.9 ± 8.5 s vs. 115.3 ± 24.8 s, $p = 0.044$; at W7: 65.5 ± 14.9 s vs. 202.1 ± 39.9 s, $p = 0.008$) (Fig. 4A). Six weeks after stroke, the postdelay task was also completed faster by the MCAo-hBM-MSC group compared to the MCAo-PBS group (180.4 ± 27.1 s vs. 266.91 ± 17.9 s, $p = 0.019$) (Fig. 4B). From 3 to 7 weeks after stroke, total errors tended to be reduced in MCAo-hBM-MSC rats (Fig. 4C) with less perseverations after 5 weeks (MCAo-hBM-MSC vs. MCAo-PBS at W5: 0.6 ± 0.2 vs. 2.0 ± 0.4, $p = 0.009$) (Fig. 4D).

IV Injection of hBM-MSCs Increased Microvascular Density

MCAo-hBM-MSC MRI and MCAo-PBS MRI groups exhibited similar values of CBV, VSI, vascular density, and BBB permeability at D7, before hBM-MSC injection (Fig. 5A–D).

At any time point, CBV and VSI were higher in both MCAo MRI groups compared to sham rats. CBV

FACING PAGE
Figure 2. (A) Persistence of human bone marrow-derived mesenchymal stem cells (hBM-MSCs) in spleen, liver, and lungs, but not in muscles after 6 weeks. Human cells in red (HuNu); nuclei in blue (Hoechst). (B–D) In the brain, few hBM-MSCs differentiated into neurons (B), astrocytes (C), or endothelial cells (D). Human nuclei in red; astrocytes (GFAP), neurons (NF200), or endothelial cells (vWF) in green. Scale bars: 50 µm.
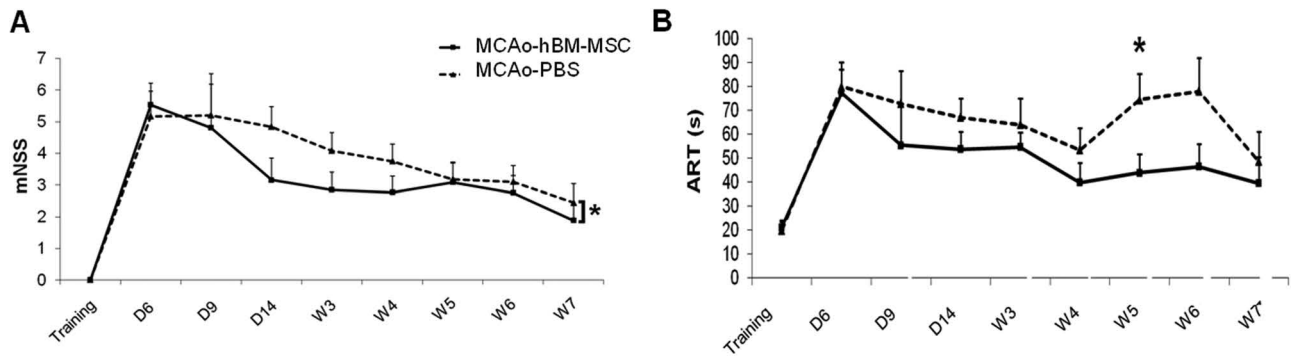
Figure 3. Sensorimotor follow-up. (A). Modified neurological severity score (mNSS), mean ± standard error of the mean (SEM); analysis of variance (ANOVA); *$p < 0.05$. (B) Left forelimb adhesive removal test (ART), mean ± SEM; *t*-test; *$p < 0.05$.

remained constant in the MCAo-hBM-MSC MRI group over the 25-day follow-up period (mean CBV: 4.4 ± 0.9%), while a significant decrease was observed in the MCAo-PBS MRI group between D16 and D25 (D16 vs. D25: 5.0 ± 0.8% vs. 3.1 ± 0.3%, $p = 0.028$). No VSI difference was observed between the MCAo MRI group until D9 (mean VSI of both MCAo groups D3–D7: 11.0 ± 1.7 µm²). VSI dropped in both groups to similar values, but this drop occurred earlier in the MCAo-hBM-MSC MRI group (at D16: 7.9 ± 1.4 µm) than in the MCAo-PBS MRI group (at D25: 6.3 ± 0.3 µm).

Vascular density in both MCAo groups was lower than in the sham group and increased until D9 (around 100 mm⁻²). Vascular density remained constant (around 120 mm⁻²) in the MCAo-PBS MRI group, while it increased in the MCAo-hBM-MSC MRI group up to a similar value to that of sham animals (D25: 158.6 ± 20.0 mm⁻² vs. 190.1 ± 44.6 mm⁻², $p = 0.329$).

At all time points, BBB permeability in the two MCAo groups was comparable. The SE following contrast agent was slightly above that of the sham (less than twofold) at all time points except at D3, where a peak
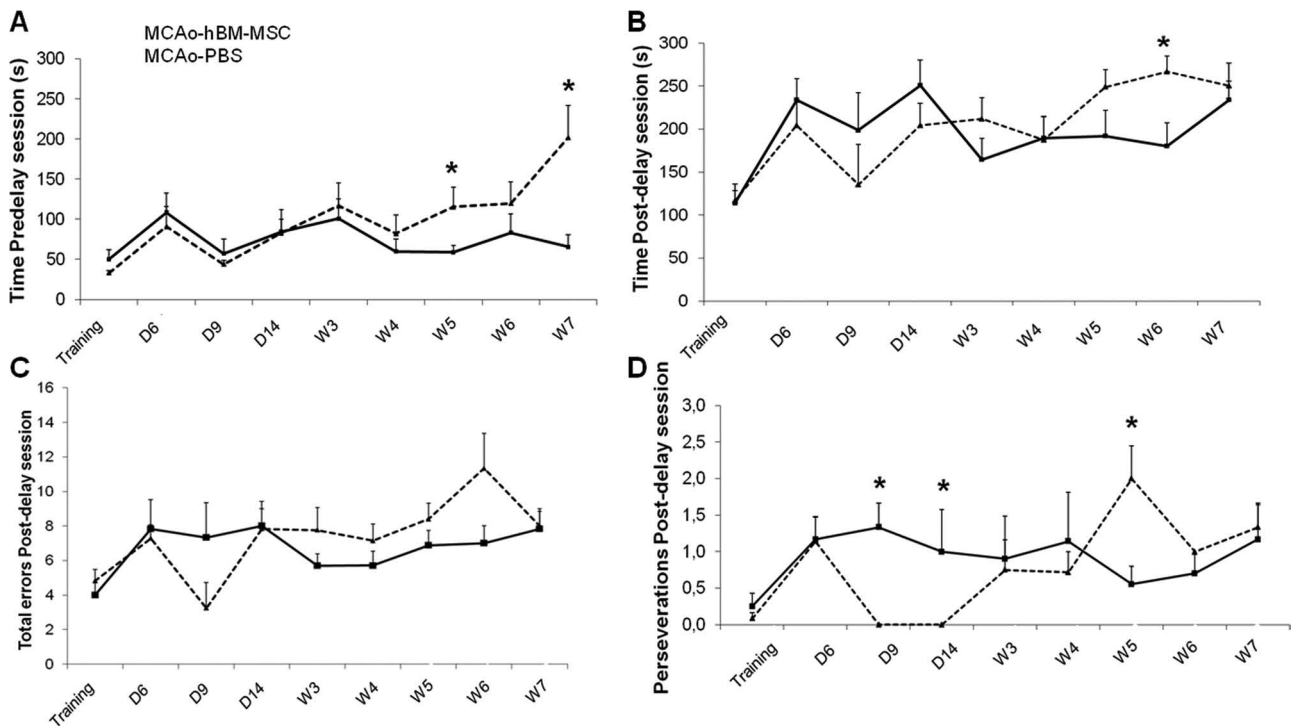

Figure 4. Cognitive follow-up. (A) Delay to encode the task during predelay session. (B) Delay to reproduce the task during postdelay session. (C) Number of total errors and perseverations (D) during the postdelay session. Mean ± SEM; *t*-test; *$p < 0.05$.
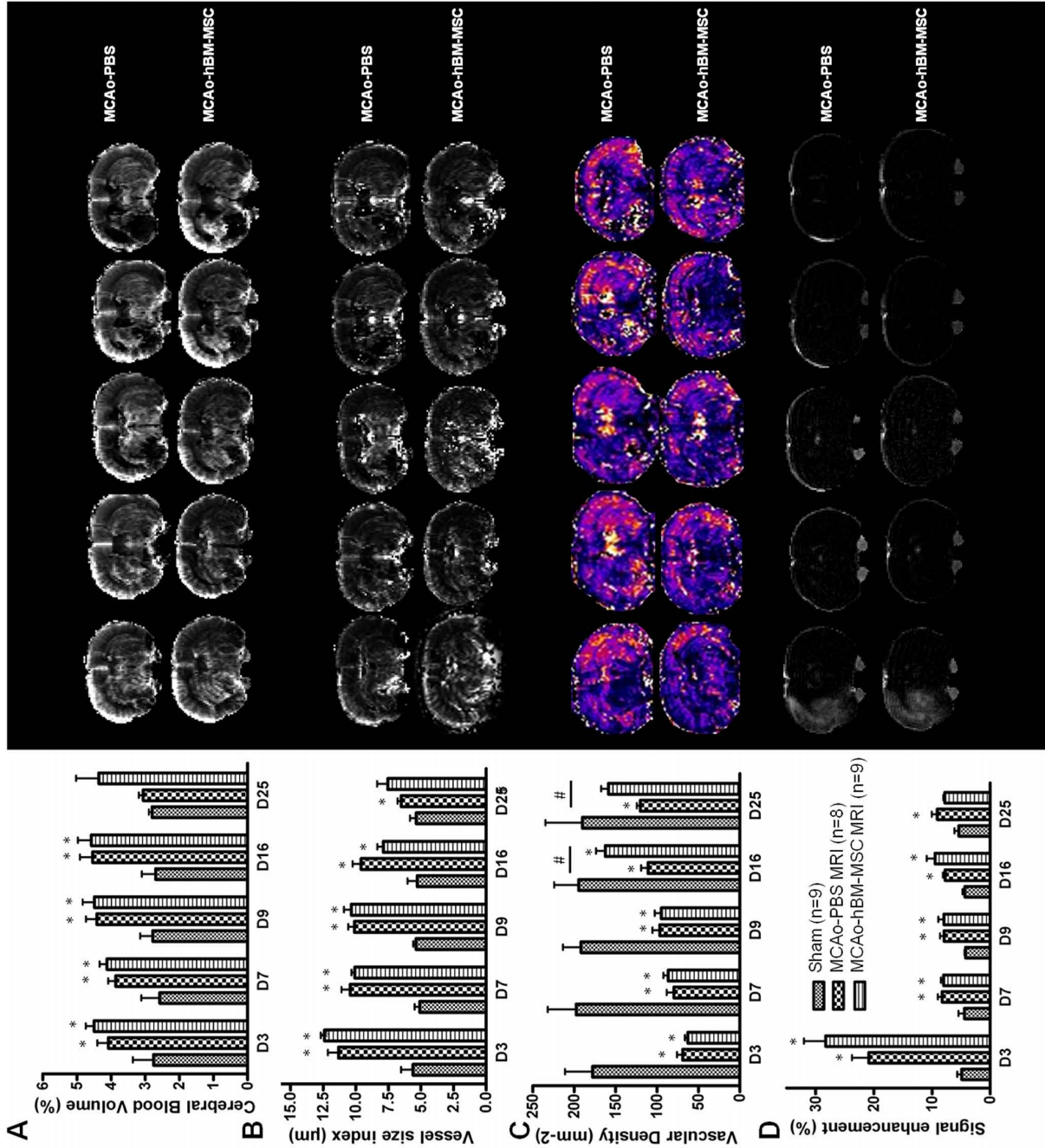
Figure 5. Evolution of (A) cerebral blood volume (CBV), (B) vessel size index (VSI), (C) vascular density, and (D) BBB permeability (signal enhancement) in MCAo-PBS MRI and MCAo-hBM-MSC MRI groups compared to sham MRI rats (mean ± standard deviation; Mann–Whitney; $*p < 0.05$) and in MCAo-PBS MRI versus MCAo-hBM-MSC MRI (Mann–Whitney; $\#p < 0.05$).

in BBB permeability was observed (more than fourfold that of sham).

IV Injection of hBM-MSCs Induced a Release of Proangiogenic Factors

Before IV injection, angiopoietin receptor 1 (*TIE1*), transforming growth factor-β1 (*TGF-β1*), and chemokine receptor type 4 (*CXCR-4*) were overexpressed at D3 and D7 in the MCAo groups compared to sham, and angiopoietin 1 (*ANG1*) was overexpressed only at D7 (Fig. 6). The other factors [*ANG2*, *TIE2*, vascular endothelial growth factor (*VEGF*), VEGF receptor-1 (*VEGFR-1*), *VEGFR-2*, stromal cell-derived factor-1 (*SDF-1*), and endothelial nitric oxide synthase (*eNOs*)] were either underexpressed or similarly expressed compared to sham rats.

One day after IV injections (D9), *ANG2*, *TGF-β1*, and *CXCR-4* were overexpressed in both MCAo MRI groups compared with sham rats, and Ang1 was overexpressed only in the MACo-hBM-MSC group.

At D16, *ANG1*, *ANG2*, and *TGF-β1* were overexpressed only in the MCAo-hBM-MSC MRI group compared to sham rats.

DISCUSSION

This study combined long-term sensorimotor and cognitive–behavioral follow-up, multiparametric MRI, and qPCR. It aimed to highlight microvascular effects and mechanisms involved in the benefits of IV-injected hBM-MSCs at the subacute stage of ischemic stroke. We showed that IV administration of hBM-MSCs induced release of endogenous angiogenic factors in the damaged hemisphere that led to a microvascular density increase over a 2-week period. One month after hBM-MSC administration, we observed sensorimotor and cognitive benefits that were sustained until at least 6 weeks postinjection. These results suggest that the impact of hBM-MSCs on microvasculature at the subacute stage of stroke might contribute to functional recovery.

Delayed IV Injection of hBM-MSCs Was Well Tolerated Despite a Whole-Body Biodistribution

In this study, behavioral follow-up of sham animals was not investigated. We have previously shown, as preliminary results (unpublished data), that IV-injected MSCs had no sensorimotor effect (mNSS and ART test) in sham animals (six MSC-sham animals vs. six PBS-sham animals). Sham-operated rats underwent the same surgery as MCAo rats without MCA occlusion (D0). We observed no significant behavioral effect in sham-operated groups before (D6) and 9 days after MSC or PBS infusion (i.e., 16 days after surgery). Regarding the ART, the mean times to remove each adhesive in MSC injection versus PBS injection groups, respectively, before treatment were as follows: 10.4±2.3 s versus 10.5±3.5 s for the right forelimb and 7.3±1.9 s versus 5.7±1.8 s for the left

forelimb, and at D16, 11.8±2.7 s versus 11.0±2.6 s and 12.9±3.7 s versus 8.8±1.3 s. NSS was equal to 0 (i.e., no deficit) for both groups at all time points.

Homing of hBM-MSCs to peripheral organs such as the spleen, liver, or lungs following IV injection has previously been reported in healthy rats, at 24/48 h[33,43] and at 13 months[44]. The presence of 0.01% to 18.5% of the IV-injected dose of hBM-MSCs has been reported in the damaged brain[3,8,9,45]. In line with these studies, we observed human cells in the brain, spleen, liver, and lungs until 6 weeks following their systemic injection. Iron cell labeling is an attractive tool to visualize migration and homing of hBM-MSCs throughout a damaged brain[46,47]. However, in the present study, it was not possible to distinguish hyposignals due to small bleeds (usually observed during the first days following cerebral infarction) from those due to SPIO particles. We preferentially visualized hBM-MSCs in the brain by histology, using HuNu labeling, rather than by MRI. Moreover, for MSC detection, SPIO (dragon green), as intracytoplasmic labeling, is unstable, and these particles can be released in vivo into the extracellular space. This may explain why ex vivo detection of human cells is better using immunohistochemistery and an HuNu antibody (Fig. 2A). We did not observe any adverse events, such as acute dyspnea or tumor formation, during the 7-week period after hBM-MSC injection. We also found that very few human cells differentiated into astrocytes, neurons, or endothelial cells in accordance with previous studies[14,15,21,26]. Thus, the transdifferentiation process cannot represent the main mechanism involved in stroke recovery induced by systemic hBM-MSC therapy, as discussed by other authors[48,49].

Delayed IV Injection of hBM-MSCs Improved Sensorimotor and Spatial Memory Recovery

When injected at the acute phase, MSCs are known to improve both sensorimotor behavior and spatial memory[3,45]. The sensorimotor recovery was also improved after IV administration of hUCB-MSCs or rat BM-MSCs at 1 week or 30 days following transient MCAo[21,22,29]. One study also reported cognitive benefits associated with delayed injection (7 days) of hBM-MSCs using an endothelin-1 stroke model[50]. In line with these previous reports, we observed sustained sensorimotor and cognitive improvements after the delayed administration of hBM-MSCs.

Human BM-MSC Injection Enhances Microvascular Plasticity

Three days after MCAo, we observed strong microvascular alterations with a decreased number of perfused vessels and predominance of enlarged vessels (high VSI). The high BBB permeability at D3 suggests destabilization of blood vessels, which is the first step
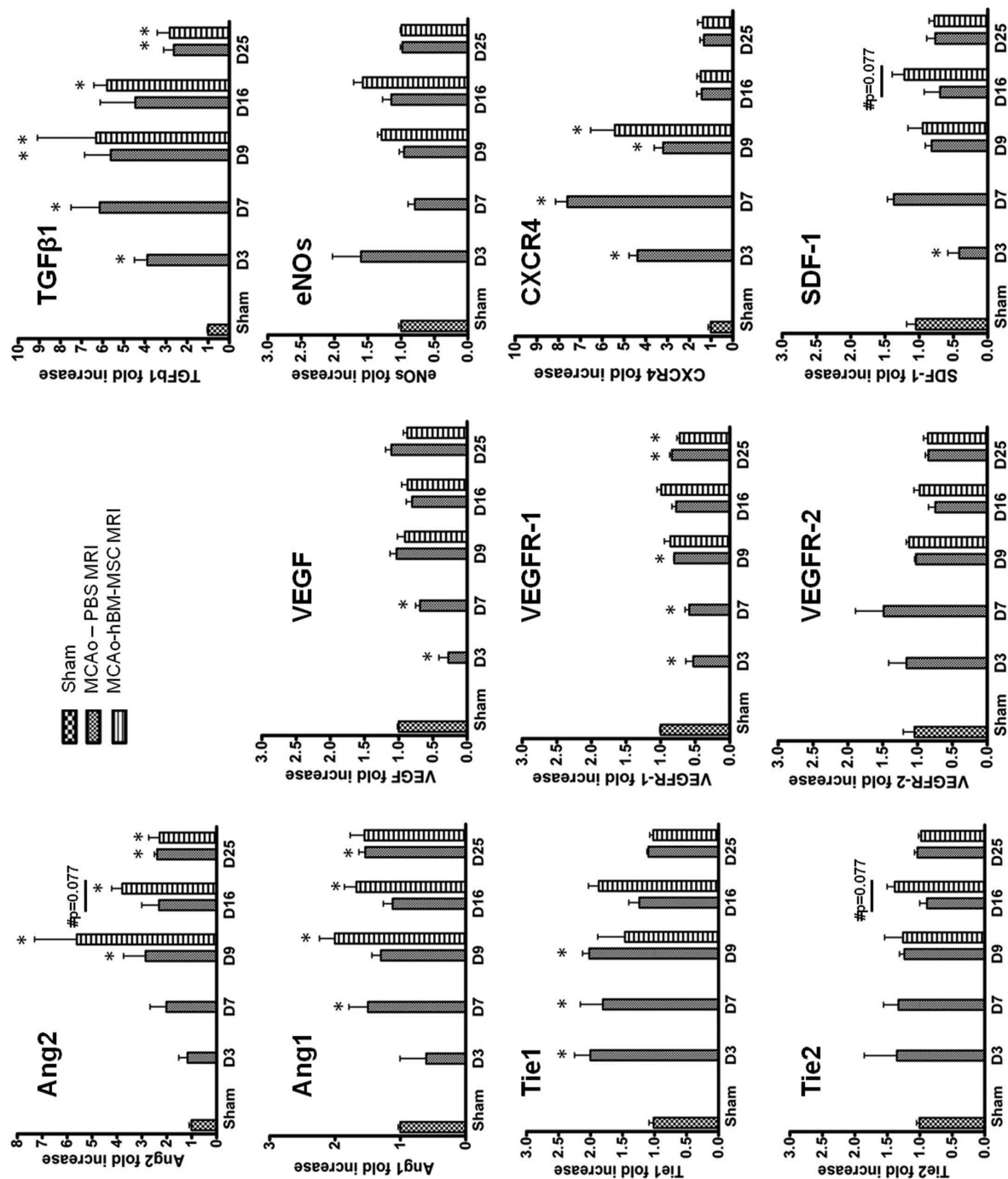
Figure 6. Expression of angiogenic factors following placebo (PBS) or human BM-MSC (hBM-MSC) IV injection after MCAo. Evolution of Ang2, Ang1, Tie1, Tie2, VEGF, VEGFR-1, VEGFR-2, TGF-β1, eNOs, SDF-1, and CXCR-4 from D1 to D25. Mean fold increase to expression in sham ± SEM of three separate experiments, two duplicates for each. MCAo versus sham (Mann–Whitney; *p < 0.05; MCAo-PBS versus MCAo-hBM-MSC (Mann–Whitney; #p = 0.077).

in the angiogenesis pathway[51]. This is in line with previous studies that reported such microvascular changes 3 days following stroke[52] or later, at 1 week[53]. Our MRI vascular changes were associated with overexpression of Tie1, TGF-β1, and CXCR-4. BBB permeability almost normalized, while vessel caliber continuously decreased until D25 and microvascular density continually increased until D16 (Fig. 5C and D). Our observations are in accordance with two other MRI studies that reported similar evolution for BBB permeability[52,54] and vascular density[52]. These delayed microvascular changes in the present study were associated with overexpression of Ang1, Ang2, Tie1, and TGF-β1 (Fig. 6). A similar increase of Ang2 and TGF-β1 has been reported in a model of transient cerebral ischemia in rats[55] and mice[56]. In accordance with Lin et al.[55], we observed an increase of Ang1 until D1, sustained until D25 in our study, although its decrease was reported by Hayashi et al.[56] between D7 and D21. Altogether, our data indicate stabilization and maturation of perfused vessels from D7 to D25[57], a process, however, insufficient to reach normal microvascular values.

IV administration of hBM-MSCs at the subacute phase (D8) accelerated the VSI decrease and perfused vessel density increase (Fig. 5B and C). These results suggest that hBM-MSCs enhance postischemic endogenous angiogenesis and microvessel maturation. Similar observations on improvement of angiogenesis have been reported after IV injection of hBM-MSCs related to a motor functional improvement[25], whereas the intracarotid injection of hBM-MSCs also showed an increase in angiogenesis in the lesion without any relation with behavioral improvement[30]. In line with this hypothesis, we observed a sustained overexpression of Ang1, Ang2, and TGF-β1 from D9 to D25 in hBM-MSC-treated rats. Overexpression of Ang1 and Ang2 has been shown in one study following early hBM-MSC IC injection with a similar evolution as ours[58]. Furthermore, 1 week after hBM-MSC injection, we showed a trend in an SDF-1 increase, in accordance with previous studies using delayed IC injection of UCB-MSCs[14] or early IV injection of ADSCs[17]. Expression levels of Ang2 and Tie2 also tend to be higher 1 week after hBM-MSC injection. In the literature, Ang2 has been shown to promote endothelial cell survival after a sustained expression[59] and participate in vascular stabilization[60] through Tie2 activation. Our results suggest a promotion of in vivo vascular stabilization by hBM-MSC therapy, in agreement with in vitro studies[61,62].

Involvement of mature and stable blood vessels in neurogenesis is now widely reported. Blood vessels contribute to neuroblast migration toward the peri-infarct "neurovascular niche" where their maturation in neurons occurs[31]. Migration of neuroblasts takes place from 2 weeks

following MCAo[63] and is induced by Ang1 and SDF-1[31], as well as Ang2[64]. Moreover, it has been reported that neuroblast maturation into neurons starts 5 weeks after ischemia and improves recovery[63]. However, only 0.2% of dead neurons after ischemia are replaced due to maturation of new neurons. Therefore, earlier overexpression of Ang1 and increased levels of SDF-1 and Ang2/Tie2, observed 1 week after delayed IV hBM-MSC injection, suggest that hBM-MSCs could enhance newborn vessel stabilization and survival. As a consequence, hBM-MSC IV injection might increase migration of neuroblasts and improve stroke recovery.

SUMMARY/CONCLUSIONS

IV injection of hBM-MSCs at the subacute stage of cerebral ischemia improves sensorimotor and spatial memory recovery. Despite being trapped in the spleen, liver, and lungs, hBM-MSCs induce angiogenic factor release, such as Ang2, Ang1, SDF-1, and TGF-β1, enhancing endogenous angiogenesis and newborn vessel stabilization. These vascular effects might contribute to the functional benefit of hBM-MSC therapy for stroke.

REFERENCES

1. Bliss T, Guzman R, Daadi M, Steinberg GK. Cell transplantation therapy for stroke. Stroke 2007;38(2 Suppl):817–26.

2. Chamberlain G, Fox J, Ashton B, Middleton J. Concise review: Mesenchymal stem cells: Their phenotype, differentiation capacity, immunological features, and potential for homing. Stem Cells 2007;25(11):2739–49.

3. Honma T, Honmou O, Iihoshi S, Harada K, Houkin K, Hamada H, Kocsis JD. Intravenous infusion of immortalized human mesenchymal stem cells protects against injury in a cerebral ischemia model in adult rat. Exp Neurol. 2006;199(1):56–66.

4. Li Y, Chen J, Chen XG, Wang L, Gautam SC, Xu YX, Katakowski M, Zhang LJ, Lu M, Janakiraman N, Chopp M. Human marrow stromal cell therapy for stroke in rat: Neurotrophins and functional recovery. Neurology 2002; 59(4):514–23.

5. Omori Y, Honmou O, Harada K, Suzuki J, Houkin K, Kocsis JD. Optimization of a therapeutic protocol for intravenous injection of human mesenchymal stem cells after cerebral ischemia in adult rats. Brain Res. 2008;1236:30–8.

6. Zheng W, Honmou O, Miyata K, Harada K, Suzuki J, Liu H, Houkin K, Hamada H, Kocsis JD. Therapeutic benefits of human mesenchymal stem cells derived from bone marrow after global cerebral ischemia. Brain Res. 2010;1310:8–16.

7. Sheikh AM, Nagai A, Wakabayashi K, Narantuya D, Kobayashi S, Yamaguchi S, Kim SU. Mesenchymal stem cell transplantation modulates neuroinflammation in focal cerebral ischemia: Contribution of fractalkine and IL-5. Neurobiol Dis. 2011;41(3):717–24.

8. Mora-Lee S, Sirerol-Piquer MS, Gutierrez-Perez M, Gomez-Pinedo U, Roobrouck VD, Lopez T, Casado-Nieto M, Abizanda G, Rabena MT, Verfaille C, Prósper F, García-Verdugo JM. Therapeutic effects of hMAPC and hMSC transplantation after stroke in mice. PLoS One 2012;7(8):e43683.

9. Chen J, Zhang ZG, Li Y, Wang L, Xu YX, Gautam SC, Lu M, Zhu Z, Chopp M. Intravenous administration of human bone marrow stromal cells induces angiogenesis in the ischemic boundary zone after stroke in rats. Circ Res. 2003;92(6):692–9.

10. Liu H, Honmou O, Harada K, Nakamura K, Houkin K, Hamada H, Kocsis JD. Neuroprotection by PlGF gene-modified human mesenchymal stem cells after cerebral ischaemia. Brain 2006;129(Pt 10):2734–45.

11. Onda T, Honmou O, Harada K, Houkin K, Hamada H, Kocsis JD. Therapeutic benefits by human mesenchymal stem cells (hMSCs) and Ang-1 gene-modified hMSCs after cerebral ischemia. J Cereb Blood Flow Metab. 2008; 28(2):329–40.

12. Toyama K, Honmou O, Harada K, Suzuki J, Houkin K, Hamada H, Kocsis JD. Therapeutic benefits of angiogenetic gene-modified human mesenchymal stem cells after cerebral ischemia. Exp Neurol. 2009;216(1):47–55.

13. Zacharek A, Chen J, Cui X, Li A, Li Y, Roberts C, Feng Y, Gao Q, Chopp M. Angiopoietin1/Tie2 and VEGF/Flk1 induced by MSC treatment amplifies angiogenesis and vascular stabilization after stroke. J Cereb Blood Flow Metab. 2007;27(10):1684–91.

14. Ding DC, Shyu WC, Chiang MF, Lin SZ, Chang YC, Wang HJ, Su CY, Li H. Enhancement of neuroplasticity through upregulation of beta1-integrin in human umbilical cord-derived stromal cell implanted stroke model. Neurobiol Dis. 2007;27(3):339–53.

15. Liao W, Xie J, Zhong J, Liu Y, Du L, Zhou B, Xu J, Liu P, Yang S, Wang J, Han Z, Han ZC. Therapeutic effect of human umbilical cord multipotent mesenchymal stromal cells in a rat model of stroke. Transplantation 2009;87(3):350–9.

16. Lin YC, Ko TL, Shih YH, Lin MY, Fu TW, Hsiao HS, Hsu JY, Fu YS. Human umbilical mesenchymal stem cells promote recovery after ischemic stroke. Stroke 2011;42(7):2045–53.

17. Leu S, Lin YC, Yuen CM, Yen CH, Kao YH, Sun CK, Yip HK. Adipose-derived mesenchymal stem cells markedly attenuate brain infarct size and improve neurological function in rats. J Transl Med. 2010;8:63.

18. Bang OY, Lee JS, Lee PH, Lee G. Autologous mesenchymal stem cell transplantation in stroke patients. Ann Neurol. 2005;57(6):874–82.

19. Lee JS, Hong JM, Moon GJ, Lee PH, Ahn YH, Bang OY. A long-term follow-up study of intravenous autologous mesenchymal stem cell transplantation in patients with ischemic stroke. Stem Cells 2010;28(6):1099–106.

20. Honmou O, Houkin K, Matsunaga T, Niitsu Y, Ishiai S, Onodera R, Waxman SG, Kocsis JD. Intravenous administration of auto serum-expanded autologous mesenchymal stem cells in stroke. Brain 2011;134(Pt 6): 1790–807.

21. Zhang L, Li Y, Zhang C, Chopp M, Gosiewska A, Hong K. Delayed administration of human umbilical tissue-derived cells improved neurological functional recovery in a rodent model of focal ischemia. Stroke 2011;42(5):1437–44.

22. Chen J, Li Y, Wang L, Zhang Z, Lu D, Lu M, Chopp M. Therapeutic benefit of intravenous administration of bone marrow stromal cells after cerebral ischemia in rats. Stroke 2001;32(4):1005–11.

23. Devasconcelos Dos Santos A, da Costa Reis J, Diaz Paredes B, Moraes L, Jasmin, Giraldi-Guimaraes A, Mendez-Otero R. Therapeutic window for treatment of cortical ischemia with bone marrow-derived cells in rats. Brain Res. 2010;1306:149–58.

24. Kawabori M, Kuroda S, Ito M, Shichinohe H, Houkin K, Kuge Y, Tamaki N. Timing and cell dose determine therapeutic effects of bone marrow stromal cell transplantation in rat model of cerebral infarct. Neuropathology 2013;33(2):140–8.

25. Komatsu K, Honmou O, Suzuki J, Houkin K, Hamada H, Kocsis JD. Therapeutic time window of mesenchymal stem cells derived from bone marrow after cerebral ischemia. Brain Res. 2010;1334:84–92.

26. Li Y, Chen J, Zhang CL, Wang L, Lu D, Katakowski M, Gao Q, Shen LH, Zhang J, Lu M, Chopp M. Gliosis and brain remodeling after treatment of stroke in rats with marrow stromal cells. Glia 2005;49(3):407–17.

27. Miyamoto M, Kuroda S, Zhao S, Magota K, Shichinohe H, Houkin K, Kuge Y, Tamaki N. Bone marrow stromal cell transplantation enhances recovery of local glucose metabolism after cerebral infarction in rats: A serial 18F-FDG PET study. J Nucl Med. 2013;54(1):145–50.

28. Ruan GP, Han YB, Wang TH, Xing ZG, Zhu XB, Yao X, Ruan GH, Wang JX, Pang RQ, Cai XM, He J, Zhao J, Pan XH. Comparative study among three different methods of bone marrow mesenchymal stem cell transplantation following cerebral infarction in rats. Neurol Res. 2013;35(2):212–20.

29. Shen LH, Li Y, Chen J, Zacharek A, Gao Q, Kapke A, Lu M, Raginski K, Vanguri P, Smith A, Chopp M. Therapeutic benefit of bone marrow stromal cells administered 1 month after stroke. J Cereb Blood Flow Metab. 2007;27(1):6–13.

30. Mitkari B, Nitzsche F, Kerkela E, Kuptsova K, Huttunen J, Nystedt J, Korhonen M, Jolkkonen J. Human bone marrow mesenchymal stem/stromal cells produce efficient localization in the brain and enhanced angiogenesis after intra-arterial delivery in rats with cerebral ischemia, but this is not translated to behavioral recovery. Behav Brain Res. 2014;259:50–9.

31. Ohab JJ, Fleming S, Blesch A, Carmichael ST. A neurovascular niche for neurogenesis after stroke. J Neurosci. 2006;26(50):13007–16.

32. Moisan A, Pannetier N, Grillon E, Richard MJ, de Fraipont F, Remy C, Barbier EL, Detante O. Intracerebral injection of human mesenchymal stem cells impacts cerebral microvasculature after experimental stroke: MRI study. NMR Biomed. 2012;25(12):1340–8.

33. Detante O, Moisan A, Dimastromatteo J, Richard MJ, Riou L, Grillon E, Barbier E, Desruet MD, De Fraipont F, Segebarth C, Jaillard A, Hommel M, Ghezzi C, Remy C. Intravenous administration of 99m Tc-HMPAO-labeled

human mesenchymal stem cells after stroke: In vivo imaging and biodistribution. Cell Transplant. 2009;18(12): 1369–79.

34. Detante O, Valable S, Fraipont FD, Grillon E, Barbier EL, Moisan A, Arnaud J, Moriscot C, Segebarth C, Hommel M, Remy C, Richard MJ. Magnetic resonance imaging and fluorescence labeling of clinical grade mesenchymal stem cells without impacting their phenotype: Study in a rat model of stroke. Stem Cells Transl Med. 2012;1:333–41.

35. Yonemori F, Yamada H, Yamaguchi T, Uemura A, Tamura A. Spatial memory disturbance after focal cerebral ischemia in rats. J Cereb Blood Flow Metab. 1996;16(5):973–80.

36. Yonemori F, Yamaguchi T, Yamada H, Tamura A. Spatial cognitive performance after chronic focal cerebral ischemia in rats. J Cereb Blood Flow Metab. 1999;19(5):483–94.

37. Tropres I, Grimault S, Vaeth A, Grillon E, Julien C, Payen JF, Lamalle L, Decorps M. Vessel size imaging. Magn Reson Med. 2001;45(3):397–408.

38. Valable S, Lemasson B, Farion R, Beaumont M, Segebarth C, Remy C, Barbier EL. Assessment of blood volume, vessel size, and the expression of angiogenic factors in two rat glioma models: A longitudinal in vivo and ex vivo study. NMR Biomed. 2008;21(10):1043–56.

39. Tropres I, Pannetier N, Grand S, Lemasson B, Moisan A, Peoc'h M, Remy C, Barbier EL. Imaging the microvessel caliber and density: Principles and applications of microvascular MRI. Magn Reson Med. 2015;73(1):325–41.

40. Wu EX, Tang H, Jensen JH. High-resolution MR imaging of mouse brain microvasculature using the relaxation rate shift index Q. NMR Biomed. 2004;17(7):507–12.

41. Lemasson B, Valable S, Farion R, Krainik A, Remy C, Barbier EL. In vivo imaging of vessel diameter, size, and density: A comparative study between MRI and histology. Magn Reson Med. 2012;69(1):18–26.

42. Schmittgen TD, Livak KJ. Analyzing real-time PCR data by the comparative C(T) method. Nat Protoc. 2008;3(6): 1101–8.

43. Gao J, Dennis JE, Muzic RF, Lundberg M, Caplan AI. The dynamic in vivo distribution of bone marrow-derived mesenchymal stem cells after infusion. Cells Tissues Organs 2001;169(1):12–20.

44. Allers C, Sierralta WD, Neubauer S, Rivera F, Minguell JJ, Conget PA. Dynamic of distribution of human bone marrow-derived mesenchymal stem cells after transplantation into adult unconditioned mice. Transplantation 2004;78(4):503–8.

45. Pavlichenko N, Sokolova I, Vijde S, Shvedova E, Alexandrov G, Krouglyakov P, Fedotova O, Gilerovich EG, Polyntsev DG, Otellin VA. Mesenchymal stem cells transplantation could be beneficial for treatment of experimental ischemic stroke in rats. Brain Res. 2008;1233:203–13.

46. Byun JS, Kwak BK, Kim JK, Jung J, Ha BC, Park S. Engraftment of human mesenchymal stem cells in a rat photothrombotic cerebral infarction model: Comparison of intra-arterial and intravenous infusion using MRI and histological analysis. J Korean Neurosurg Soc. 2013;54(6): 467–76.

47. Tarulli E, Chaudhuri JD, Gretka V, Hoyles A, Morshead CM, Stanisz GJ. Effectiveness of micron-sized superparamagnetic iron oxide particles as markers for detection of migration of bone marrow-derived mesenchymal stromal cells in a stroke model. J Magn Reson Imaging 2013;37(6):1409–18.

48. da Silva Meirelles L, Sand TT, Harman RJ, Lennon DP, Caplan AI. MSC frequency correlates with blood vessel density in equine adipose tissue. Tissue Eng Part A 2009; 15(2):221–9.

49. Borlongan CV, Hadman M, Sanberg CD, Sanberg PR. Central nervous system entry of peripherally injected umbilical cord blood cells is not required for neuroprotection in stroke. Stroke 2004;35(10):2385–9.

50. Lowrance SA, Fink KD, Crane A, Matyas J, Dey ND, Matchynski JJ, Thibo T, Reinke T, Kippe J, Hoffman C, Sandstrom M, Rossignol J, Dunbar GL. Bone-marrow-derived mesenchymal stem cells attenuate cognitive deficits in an endothelin-1 rat model of stroke. Restor Neurol Neurosci. 2013;33(4):579–88.

51. Risau W. Mechanisms of angiogenesis. Nature 1997;386 (6626):671–4.

52. Lin CY, Chang C, Cheung WM, Lin MH, Chen JJ, Hsu CY, Chen JH, Lin TN. Dynamic changes in vascular permeability, cerebral blood volume, vascular density, and size after transient focal cerebral ischemia in rats: Evaluation with contrast-enhanced magnetic resonance imaging. J Cereb Blood Flow Metab. 2008;28(8):1491–501.

53. Boehm-Sturm P, Farr TD, Adamczak J, Jikeli JF, Mengler L, Wiedermann D, Kallur T, Kiselev V, Hoehn M. Vascular changes after stroke in the rat: A longitudinal study using optimized magnetic resonance imaging. Contrast Media Mol Imaging 2013;8(5):383–92.

54. Strbian D, Durukan A, Pitkonen M, Marinkovic I, Tatlisumak E, Pedrono E, Abo-Ramadan U, Tatlisumak T. The blood-brain barrier is continuously open for several weeks following transient focal cerebral ischemia. Neuroscience 2008;153(1):175–81.

55. Lin TN, Wang CK, Cheung WM, Hsu CY. Induction of angiopoietin and Tie receptor mRNA expression after cerebral ischemia-reperfusion. J Cereb Blood Flow Metab. 2000;20(2):387–95.

56. Hayashi T, Noshita N, Sugawara T, Chan PH. Temporal profile of angiogenesis and expression of related genes in the brain after ischemia. J Cereb Blood Flow Metab. 2003; 23(2):166–80.

57. Moisan A, Favre IM, Rome C, Grillon E, Naegele B, Barbieux M, De Fraipont F, Richard MJ, Barbier EL, Remy C, Detante O. Microvascular plasticity after experimental stroke: A molecular and MRI study. Cerebrovasc Dis. 2014;38(5):344–53.

58. Ma XL, Liu KD, Li FC, Jiang XM, Jiang L, Li HL. Human mesenchymal stem cells increases expression of alpha-tubulin and angiopoietin 1 and 2 in focal cerebral ischemia and reperfusion. Curr Neurovasc Res. 2013;10(2):103–11.

59. Kim I, Kim JH, Moon SO, Kwak HJ, Kim NG, Koh GY. Angiopoietin-2 at high concentration can enhance endothelial cell survival through the phosphatidylinositol 3'-kinase/Akt signal transduction pathway. Oncogene 2000;19(39):4549–52.

60. Teichert-Kuliszewska K, Maisonpierre PC, Jones N, Campbell AI, Master Z, Bendeck MP, Alitalo K, Dumont DJ, Yancopoulos GD, Stewart DJ. Biological action of angiopoietin-2 in a fibrin matrix model of angiogenesis is associated with activation of Tie2. Cardiovasc Res. 2001;49(3):659–70.

61. Duffy GP, Ahsan T, O'Brien T, Barry F, Nerem RM. Bone marrow-derived mesenchymal stem cells promote angiogenic processes in a time- and dose-dependent manner in vitro. Tissue Eng Part A 2009;15(9):2459–70.

62. Sorrell JM, Baber MA, Caplan AI. Influence of adult mesenchymal stem cells on in vitro vascular formation. Tissue Eng Part A 2009;15(7):1751–61.

63. Arvidsson A, Collin T, Kirik D, Kokaia Z, Lindvall O. Neuronal replacement from endogenous precursors in the adult brain after stroke. Nat Med. 2002;8(9):963–70.

64. Liu XS, Chopp M, Zhang RL, Hozeska-Solgot A, Gregg SC, Buller B, Lu M, Zhang ZG. Angiopoietin 2 mediates the differentiation and migration of neural progenitor cells in the subventricular zone after stroke. J Biol Chem. 2009;284(34):22680–9.